JOURNAL OF OPTOELECTRONICS AND ADVANCED MATERIALS Vol. 10, No. 1, January 2008, p. 66 - 73

Structural investigations of some Bi_2O_3 based glasses

I. ARDELEAN*, D. RUSU
Faculty of Physics, Babes-Bolyai University, 400084 Cluj – Napoca, Romania

A comparative structural study was made on the glass systems $xFe_2O_3 \cdot (100-x)Bi_2O_3$ and $xFe_2O_3 \cdot (100-x)[Bi_2O_3 \cdot MO]$ (where MO => CdO, As_2O_3 and GeO_2), with $0 \le x \le 50$ mol%. The samples were prepared and investigated by X – ray diffraction, FT – IR and Raman spectroscopies in order to determine their local structure. From FT – IR spectra it can be observed that, in all studied oxide matrices, the predominant structural units are those characteristic to Bi_2O_3 and also some structural units characteristic to As_2O_3, GeO_4 and Fe_2O_3 were evidenced. The Raman spectra confirm the structure proposed by FTIR. By both, FT – IR and Raman spectroscopies, it can be observed that the controlled dopping with iron ions induce some structural changes in the glass matrices.

(Received September 25, 2007; accepted January 10, 2008)

Keywords: Bi_2O_3 based glasses, Iron ions, X-ray diffraction, FTIR; Raman

1. Introduction

During recent years, there has been an increasing interest in the synthesis and investigation of the structure and physical properties of heavy metal oxide glasses containing Bi_2O_3, due to their high refractive index, high IR transparency and high third order non-linear optical susceptibility [1, 2]. Due to these properties, the bismuthate glasses have wide applications in the field of glass ceramics, layers for optical and optoelectronic devices, thermal and mechanical sensors and reflecting windows [1]. Also, the interest in these glasses has increased because their suitability to synthesize high – temperature ceramic superconductors [3]. Dumbaugh et al. [4] concluded that these properties usually come at the expense of glass stability. They studied the glass forming regions of heavy metal oxides (HMO) such as Bi_2O_3 by adding several oxides as CdO, As_2O_3 and GeO_2 [4] due to their properties such as those mentioned below. CdO is thermally stable, sublime and appreciably covalent [5]. As_2O_3 is a network former with corner – sharing AsO_3 pyramidal units [6]. As_2O_3 based glasses have been identified as the low-loss materials for long-distance optical transmission [7]. These glasses have exceptionally high transmission potential in the far infrared region when compared with the conventional glasses based on B_2O_3, SiO_2, P_2O_5 and GeO_2. They have very high Raman scattering coefficients and are found to be suitable for active fiber Raman amplification [8]. GeO_2 is a typical glass former [9] and germanate glasses have potential use as optical fibers and infrared transmitting windows [10].

Transition metal ions are being extensively used in the present day to probe the glass structure, since their outer d – electron orbital functions have broad radial distribution and due to their high sensitive response to the changes in the surrounding actions [11]. Among various transition metal ions, iron ions have strong bearing on electrical, optical and magnetic properties [12]. The addition of iron ions in the Bi_2O_3 based vitreous network may confer to the investigated glasses semiconducting properties [13].

The aim of the present study was to obtain, by means of FT – IR and Raman spectroscopies, information regarding the local structure of $xFe_2O_3 \cdot (100-x)Bi_2O_3$ and $xFe_2O_3 \cdot (100-x)[Bi_2O_3 \cdot MO]$glass systems (where MO => CdO, As_2O_3 and GeO_2) and to point out the role of every component in the forming of the glass structure.

2. Experimental procedures

$xFe_2O_3 \cdot (100-x)Bi_2O_3$ and $xFe_2O_3 \cdot (100-x)[Bi_2O_3 \cdot MO]$ systems (where MO => CdO, As_2O_3 and GeO_2) were prepared by mixing components of reagent grade purity, $Bi(NO_3)_3 \cdot 5H_2O$, $CdCO_3$, As_2O_3, GeO_2 and Fe_2O_3, in suitable proportions to obtain the desired compositions. The mixtures were melted in sintered corundum crucibles, introduced in an electric furnace Carbolite RF 1600, directly at 1250° C and kept for 5 minutes at this temperature. They were quickly cooled at room temperature by pouring onto stainless steel plates.

The structure of samples was analyzed by means of X-ray diffraction, using powders, with a Bruker D8 Advanced diffractometer. As reference the latest database of ICDD – International Center for Diffraction Data was used.

The FT – IR spectra have been recorded using a Bruker Equinox 55 with a spectral range from 4000 cm^{-1} to 370 cm^{-1}. A MIR, GLOBAR generator cooled with air was used. The detection was carried out with a DLATGS detector with a KBr window. The spectral resolution was about 0.5 cm^{-1}. The samples were prepared using KBr pellet technique. Due to the fact that the characteristic bands of the investigated glasses were found below 1000 cm^{-1}, it was decided to represent the FT – IR spectra only in the region 1000 – 400 cm^{-1}.

The Raman spectra were recorded, on bulk samples, at room temperature using an integrated FRA 106/S Raman module attached to Bruker Equinox 55 with a spectral

range from 3600 cm^{-1} to 70 cm^{-1}. An Nd:YAG laser with an output power of 500 mW and an 1064 nm radiation was used. The detection was carried out with an ultrasensitive D418-T detector cooled with liquid nitrogen. The spectral resolution was about 1 cm^{-1}.

3. Results and discussions

a) FT – IR spectra of Bi_2O_3 and Bi_2O_3·MO (where MO => CdO, As_2O_3 and GeO_2) glass matrices

FT – IR spectra of crystalline Bi_2O_3 and Bi_2O_3·MO (where MO => CdO, As_2O_3 and GeO_2) glass matrices are presented in Fig. 1. The spectra were discussed on the basis of the method given by Tarte [14] and Condrate [15] by comparing the experimental data of glasses with those of related crystalline compounds. In this case the infrared absorption spectra of α – Bi_2O_3, Bi_2O_3 [16 – 18], CdO [19], As_2O_3 [20, 21] and GeO_2 [10] oxides in vitreous and crystalline phase were used.

- The FT – IR spectrum of α – Bi_2O_3 presents eight absorption bands at ~ 670 cm^{-1}, ~ 620 cm^{-1} [9], ~ 595 cm^{-1}, ~ 540 cm^{-1}, ~ 510 cm^{-1}, ~ 465 cm^{-1}, ~ 425 cm^{-1} and ~ 380 cm^{-1} [16 – 18] interpreted as vibrations of Bi – O bonds of different lengths in the distorted BiO_6 octahedral units, while for Bi_2O_3 spectrum four absorption bands were identified at ~ 840 cm^{-1}, ~ 620 – 540 cm^{-1}, ~ 470 cm^{-1} and ~ 350 cm^{-1} characteristic to the vibrations of Bi – O bonds of BiO_3 pyramidal units as it follows: totally symmetric stretching vibrations at ~ 840 cm^{-1}, doubly degenerate stretching vibrations at ~ 620 – 540 cm^{-1}, totally symmetric bending vibrations at ~ 470 cm^{-1} and doubly degenerate bending vibrations at ~ 350 cm^{-1} [9, 16 – 18, 22]. Also two new bands were mentioned in literature at ~ 732 cm^{-1} due to the Bi – O symmetrical stretching vibrations in BiO_3 units and ~ 890 cm^{-1} due to vibrations of Bi – O bonds in distorted BiO_6 units [23].
- CdO does not present any absorption bands in the region ~ 250 – 750 cm^{-1} [19].
- In the FT – IR spectrum of crystalline As_2O_3 four prominent bands have been observed and identified as ν_1 (1050 cm^{-1}) – totally symmetric stretching vibrations; ν_2 (625 cm^{-1}) –totally symmetric bending vibrations; ν_3 (812 cm^{-1}) – doubly degenerate stretching vibrations and ν_4 (495 cm^{-1}) –doubly degenerate bending vibrations of AsO_3 structural units [20, 21].
- The FT – IR spectrum of vitreous GeO_2 presents four bands: a maximum absorption at ~ 915 cm^{-1} assigned to the asymmetric stretching vibrations ν_{as} of Ge (4) – O – Ge (4) bridges, a maximum absorption at ~ 750 cm^{-1} assigned to the asymmetric stretching vibrations ν_{as} of Ge – O^- bonds, a week band at ~ 585 cm^{-1} assigned to the bending vibrations of Ge (4) – O – Ge (4) bridges and a band at ~ 315 cm^{-1} attributed to a rocking motion of the bridging oxygen atom perpendicular to the Ge – O – Ge plane [10].

In our case, the experimental FT – IR spectrum of crystalline Bi_2O_3 presents the following absorption bands at ~ 874 cm^{-1}, ~ 845 cm^{-1}, ~ 668 cm^{-1}, ~ 601 cm^{-1}, ~ 541 cm^{-1}, ~ 500 cm^{-1} and ~ 421 cm^{-1} (Fig.1). The band from ~ 874 cm^{-1} is due to vibrations of Bi – O bonds in distorted BiO_6 units [23]. The band from ~ 845 cm^{-1} is due to the symmetrical stretching vibrations of Bi – O bonds in BiO_3 groups [9, 16 – 18]. The bands from ~ 668 cm^{-1}, ~ 601 cm^{-1}, ~ 541 cm^{-1}, ~ 500 cm^{-1} and ~ 421 cm^{-1} are interpreted as vibrations of Bi – O bonds of different lengths in BiO_6 polyhedra [9, 16 – 18]. The network structure proposed for Bi_2O_3 is formed from BiO_6 polyhedra with terminal links in BiO_3 polyhedra.

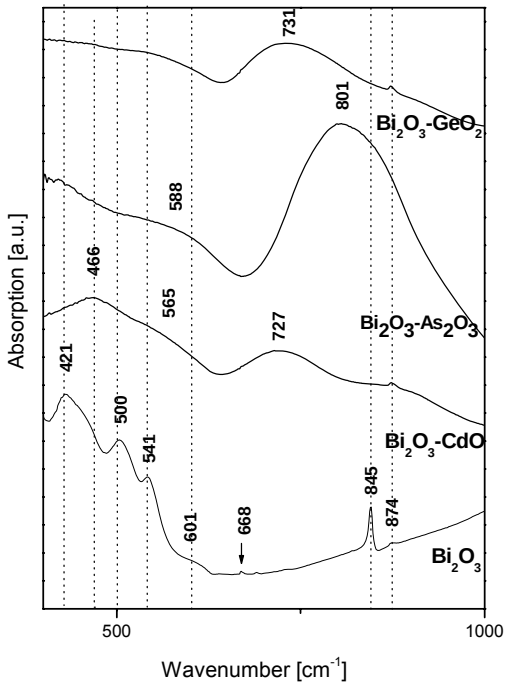

Fig. 1. FT – IR spectra of Bi_2O_3 and Bi_2O_3·MO (where MO => CdO, As_2O_3 and GeO_2) glass matrices.

The FT – IR spectrum of Bi_2O_3·CdO glass matrix presents four absorption bands at: ~ 874 cm^{-1}, ~ 727 cm^{-1}, ~ 565 cm^{-1} and ~ 465 cm^{-1}. The band from ~ 874 cm^{-1} is interpreted as vibrations of Bi – O bonds of different lengths in BiO_6 polyhedra [23]. The band from ~ 727 cm^{-1} is due to the Bi – O symmetrical stretching vibrations in BiO_3 units [23]. The band from ~ 565 cm^{-1} is due to doubly degenerate stretching vibrations of Bi – O bonds from BiO_6 groups [9, 17, 22]. The band from ~ 465 cm^{-1} is due to totally symmetric bending vibrations of Bi – O bonds from BiO_6 groups [9, 17, 22]. It can be observed that the presence of CdO in the glass matrix favorite the appearance of BiO_3 structural units. Also, due to the appearance of new broad bands comparing with those observed from Bi_2O_3 spectrum, it can be concluded that CdO changes the local symmetry in BiO_6 and BiO_3

polyhedra and implicit in the glass network structure and implies a certain disorder degree in the structure.

The FT – IR spectrum of $Bi_2O_3 \cdot As_2O_3$ glass matrix presents three absorption bands at: ~ 801 cm^{-1}, ~ 588 cm^{-1} and ~ 421 cm^{-1}. The band from ~ 801 cm^{-1}can be assigned to doubly degenerate stretching vibrations of some As – O bonds [20, 21]. Due to its broadness and asymmetric shape, the contribution on this band of the vibrations of Bi – O bonds of different lengths in BiO_6 polyhedra [9, 17] and the symmetrical stretching vibrations of Bi – O bonds in BiO_3 groups [9, 17] can not be excluded. The broad band centered at ~ 588 cm^{-1} can be assigned to totally symmetric bending vibrations of some As – O [20, 21] over which the vibrations of Bi – O bonds of BiO_6 polyhedra can be superposed. The band from ~ 421 cm^{-1} is interpreted as vibrations of Bi – O bonds of different lengths in BiO_6 polyhedra [9, 17]. These results suggest a competitive role between Bi_2O_3 and As_2O_3 as glass former. A conclusion in this matter can not be draw due to the broadness and asymmetric shape of the bands which suggest a superposition of several bands due to both oxides.

The FT – IR spectrum of $Bi_2O_3 \cdot GeO_2$ glass matrix presents three absorption bands at: ~ 874 cm^{-1}, ~ 731 cm^{-1} and ~ 565 cm^{-1}. The band from ~874 cm^{-1} is interpreted as vibrations of Bi – O bonds of different lengths in BiO_6 polyhedra [23]. The band from ~ 731 cm^{-1} is due to the Bi – O symmetrical stretching vibrations in BiO_3 units [23] over which the contribution of the asymmetric stretching vibrations ν_{as} of Ge – O^- bonds van not be excluded [10]. The band from ~ 565 cm^{-1} is due to doubly degenerate stretching vibrations of Bi – O bonds from BiO_6 groups [9, 17, 22] over which can be superposed the bending vibrations of Ge (4) – O – Ge (4) bridges [10]. It can be observed that the presence of GeO_2 in the glass matrix favorite the appearance of BiO_3 structural units. Due to the appearance of new broad bands comparing with those observed from Bi_2O_3 spectrum, it can be concluded that GeO_2 changes the local symmetry in BiO_6 and BiO_3 polyhedra and implicit in the glass network structure.

It can be remarked that the FT – IR absorption of these vitreous matrices depends of their structure and the nature of the vitreous network modifiers (CdO, As_2O_3 or GeO_2).

b) Raman spectra of Bi_2O_3 and $Bi_2O_3 \cdot MO$ (where MO ⟹ CdO, As_2O_3 and GeO_2) glass matrices

Raman spectra of crystalline Bi_2O_3 and $Bi_2O_3 \cdot MO$ (where MO ⟹ CdO, As_2O_3 and GeO_2) glass matrices are presented in Fig. 2.

The Raman bands are discussed on the basis of the theory given by Lines et al. [24, 25]. They interpreted the Raman bands as being of four types: acoustic Raman (AR) peaks in the low frequency region (less than 100 cm^{-1}); heavy metal (HM) peaks in the region 70-160 cm^{-1}; bridged anion (BA) peaks in the intermediate region (300-600 cm^{-1}) and non – bridged anion (NBA) peaks at higher frequencies.

The Raman experimental spectrum of crystalline Bi_2O_3 can be divided in three regions (Fig. 2):

- 0 – 300 cm^{-1} – The bands from this region are assumed to be derived from both AR and HM modes [21].
- 300 – 600 cm^{-1} – The bands from this region are assigned to symmetric stretching anion motion in an angulary constrained Bi – O – Bi configuration from BiO_6 octahedral units [26]
- 600 – 1000 cm^{-1} – The band from ~ 694 cm^{-1} is assigned to Bi – O^- stretching vibrations of BiO_6 octahedral units [22, 26].

The experimental Raman spectrum of $Bi_2O_3 \cdot CdO$ glass matrix presents two bands at ~ 406 cm^{-1} and ~ 123 cm^{-1}. The broad band centered at ~ 406 cm^{-1} is assigned to symmetric stretching anion motion in an angulary constrained Bi – O – Bi configuration from BiO_6 octahedral units [26]. The broadening of this band is due to the disorder induced by the presence of CdO. The band from ~ 123 cm^{-1} is assumed to be derived from both AR and HM modes [27]. It can be noticed that this glass matrix has the most disordered structure, reported to $Bi_2O_3 \cdot As_2O_3$ and $Bi_2O_3 \cdot GeO_2$ matrices.

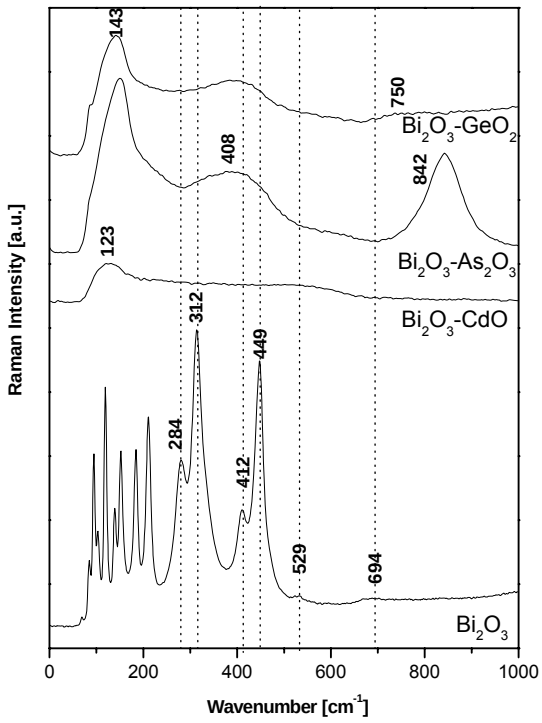

Fig. 2. Raman spectra of Bi_2O_3 and $Bi_2O_3 \cdot MO$ (where MO ⟹ CdO, As_2O_3 and GeO_2) glass matrices.

The Raman spectrum of $Bi_2O_3 \cdot As_2O_3$ glass matrix presents three bands at ~ 842 cm^{-1}, ~ 408 cm^{-1} and ~ 143 cm^{-1}. The band from ~ 842 cm^{-1} is assigned to As – O – As stretching vibrations [28]. The broad band centered at ~ 408 cm^{-1} is assigned to symmetric stretching anion motion

in an angulary constrained Bi – O – Bi configuration from BiO_6 octahedral units [26]. The band from ~ 143 cm^{-1} is assumed to be derived from both AR and HM modes [27]. The Raman spectra confirm the competitive role between Bi_2O_3 and As_2O_3 as glass former.

The Raman spectrum of $Bi_2O_3 \cdot GeO_2$ glass matrix presents three bands at ~ 750 cm^{-1}, ~ 408 cm^{-1} and ~ 143 cm^{-1}. The band from ~ 750 cm^{-1} is assigned to the characteristic vibration modes of GeO_4 tetrahedral units [29]. The broad band centered at ~ 408 cm^{-1} is assigned to symmetric stretching anion motion in an angulary constrained Bi – O – Bi configuration from BiO_6 octahedral units [26]. Over this band the symmetric stretch motion of Ge-O-Ge bridges between GeO_4 octahedra can be superposed [30]. The band from ~ 143 cm^{-1} is assumed to be derived from both AR and HM modes [27].

From Raman spectra it can be observed a broadening of the bands in all vitreous matrices due to the disorderness of the structure. The disorder degree depends of the nature of the vitreous network modifiers (CdO, As_2O_3 or GeO_2), so it can be remarked that $Bi_2O_3 \cdot CdO$ glass matrix has the most disordered structure from the other glass matrices studied.

c) Structural investigations of $xFe_2O_3 \cdot (100-x)Bi_2O_3$ and $xFe_2O_3 \cdot (100-x)[Bi_2O_3 \cdot MO]$ systems (where MO ⇒ CdO, As_2O_3 and GeO_2)

3.1. X – ray diffraction data

The XRD patterns of $xFe_2O_3 \cdot (100-x)Bi_2O_3$ and $xFe_2O_3 \cdot (100-x)[Bi_2O_3 \cdot MO]$ (where MO ⇒ CdO, As_2O_3 and GeO_2) systems, for x ≥ 35 mol%, are presented in Fig. 3.

The XRD patterns obtained for $xFe_2O_3 \cdot (100-x)Bi_2O_3$ and $xFe_2O_3 \cdot (100-x)[Bi_2O_3 \cdot CdO]$ systems present a broad diffuse scattering at low angles which indicates a long – range structural disorder characteristic to vitreous solids up to 35 mol% Fe_2O_3. From XRD patterns of $xFe_2O_3 \cdot (100-x)Bi_2O_3$ system, it can be observed (Fig. 3) that the samples with x ≥ 35 mol% present a crystalline phase which was detected and identified as $Bi(FeO_3)$. From XRD patterns of $xFe_2O_3 \cdot (100-x)[Bi_2O_3 \cdot CdO]$ system it can be observed that, for x ≥ 35 mol%, the vitreous and the crystalline phase coexist. They were identified as $Bi_{1.5}Cd_{0.5}O_{2.75}$ and Fe_3O_4. Because this study is referring to glass systems, only the samples from 0 to 20 mol% Fe_2O_3, for both systems, will be discussed afterwards.

The XRD patterns obtained for $xFe_2O_3 \cdot (100-x)(Bi_2O_3 \cdot As_2O_3)$ and $xFe_2O_3 \cdot (100-x)(Bi_2O_3 \cdot GeO_2)$ systems present a broad diffuse scattering at low angles, which indicates a long – range structural disorder characteristic to vitreous solids up to 50 mol% Fe_2O_3.

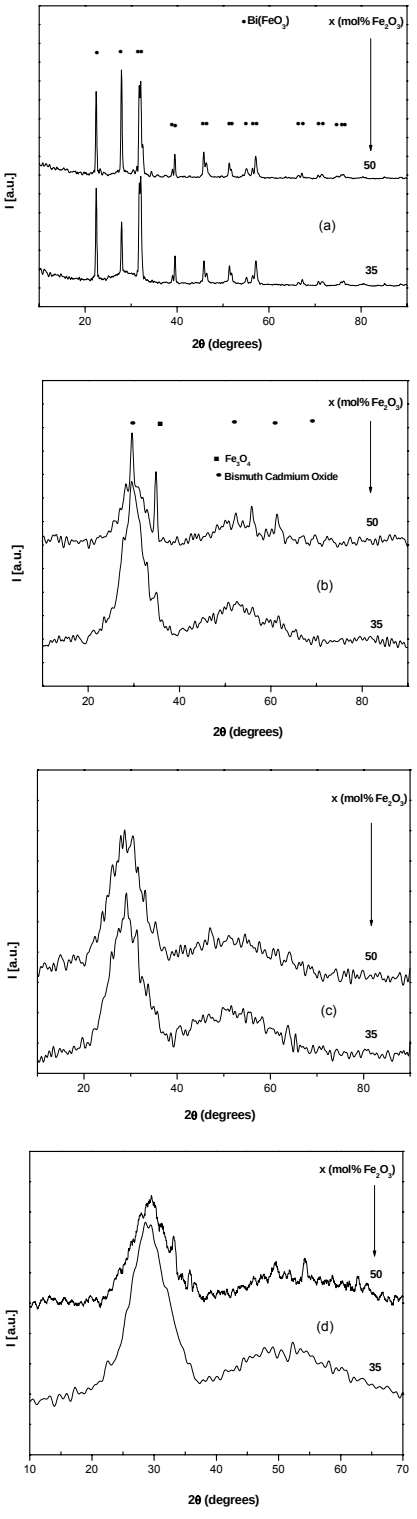

Fig. 3. XRD patterns of (a) $xFe_2O_3 \cdot (100-x)Bi_2O_3$, (b) $xFe_2O_3 \cdot (100-x)[Bi_2O_3 \cdot CdO]$, (c) $xFe_2O_3 \cdot (100-x)[Bi_2O_3 \cdot As_2O_3]$ and (d) $xFe_2O_3 \cdot (100-x)[Bi_2O_3 \cdot GeO_2]$ systems for x ≥ 35 mol%.

The data obtained by X – ray diffraction suggest that, with the increasing of the valence state of the glass modifiers (Fe^{3+}or/and Fe^{2+}, Cd^{2+}, As^{3+}, Ge^{4+}), the network structure tend to be more disordered. This can be stated by the forming of a vitreous state for $x \leq 20$ mol% in $xFe_2O_3 \cdot (100\text{-}x)Bi_2O_3$ and $xFe_2O_3 \cdot (100\text{-}x)[Bi_2O_3 \cdot CdO]$ systems and for $x \leq 50$ mol% in $xFe_2O_3 \cdot (100\text{-}x)(Bi_2O_3 \cdot As_2O_3)$ and $xFe_2O_3 \cdot (100\text{-}x)(Bi_2O_3 \cdot GeO_2)$ systems.

3.2. FT – IR absorption data

The infrared absorption spectra obtained for $xFe_2O_3 \cdot (100\text{-}x)Bi_2O_3$ and $xFe_2O_3 \cdot (100\text{-}x)[Bi_2O_3 \cdot MO]$ (where MO ⟹ CdO, As_2O_3 and GeO_2) are presented in figure 4. In this case the FT – IR spectrum of vitreous Fe_2O_3 was used as a reference [17]. In pure Fe_2O_3 the characteristic vibrations of Fe – O in FeO_4 groups and ferrite compounds are at ~ 660 and ~ 625 cm^{-1}, while the vibrations of Fe – O in FeO_6 they are at ~ 580 – 550 and ~ 470 cm^{-1} [17].

The FT – IR spectra of $xFe_2O_3 \cdot (100\text{-}x)Bi_2O_3$ glass system present four absorption bands corresponding to the following wavenumber: ~ 874 cm^{-1}, ~ 855 cm^{-1}, ~ 727 cm^{-1}, ~ 669 cm^{-1}, ~ 549 cm^{-1} and ~ 465 cm^{-1} (Fig. 4). The band from ~ 874 cm^{-1} is interpreted as vibrations of Bi – O bonds of different lengths in BiO_6 polyhedra [23]. The band from ~ 845 cm^{-1} is due to the symmetrical stretching vibrations of Bi – O bonds in BiO_3 groups [9, 16 – 18]. The band from ~ 727 cm^{-1} is due to the Bi – O symmetrical stretching vibrations in BiO_3 units [23]. These bands are decreasing with the increasing of iron content. The band from ~ 668 cm^{-11} is due to the vibrations of Bi – O bonds of different lengths in BiO_6 polyhedra [9, 16 – 18]. Also, the contribution band of the vibrations of Fe – O bonds of FeO_4 units [16, 17] cannot be excluded. This band remains unchanged in all compositional range. The band from ~ 549 cm^{-1} is due to doubly degenerate stretching vibrations of Bi – O bonds from BiO_6 groups [9, 17, 22]. The band from ~ 465 cm^{-1} is due to totally symmetric bending vibrations of Bi – O bonds from BiO_6 groups [9, 17, 22]. Over the bands from ~ 465 cm^{-1} and ~ 549 cm^{-1} the vibrations of Fe – O bonds from FeO_6 units can be superposed [16, 17]. These bands are increasing with the increasing of iron content. The structure proposed from FT – IR absorption spectra is mainly based on BiO_6 and BiO_3 units. The increasing of iron content causes a decreasing of the number of BiO_6 and BiO_3 units and probably the increasing of the number of the FeO_6 units.

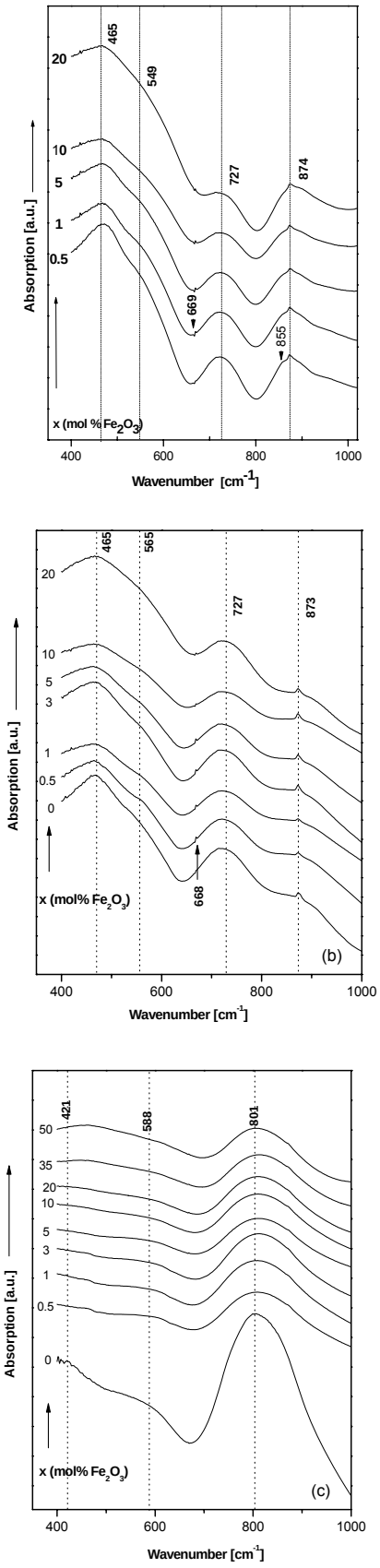

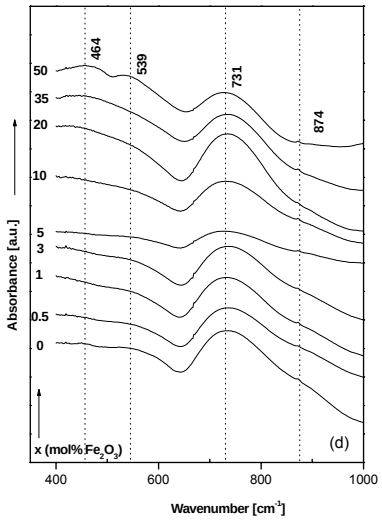

Fig. 4. FT – IR spectra of (a) $xFe_2O_3 \cdot (100\text{-}x)Bi_2O_3$, (b) $xFe_2O_3 \cdot (100\text{-}x)[Bi_2O_3 \cdot CdO]$ systems for x ≤ 20 mol% and (c) $xFe_2O_3 \cdot (100\text{-}x)[Bi_2O_3 \cdot As_2O_3]$, (d) $xFe_2O_3 \cdot (100\text{-}x)[Bi_2O_3 \cdot GeO_2]$ systems for x ≤ 50 mol%.

The FT – IR spectra of $xFe_2O_3 \cdot (100\text{-}x)[Bi_2O_3 \cdot CdO]$ glass system were studied starting from the FT – IR spectrum of $Bi_2O_3 \cdot CdO$ glass matrix presented in Fig. 1. The addition and increasing of iron content (Fig. 4) in the glass matrix causes a slowly decreasing of the bands from ~ 873 cm^{-1} and ~ 727 cm^{-1}. The shape and the intensity of the bands from ~ 557 cm^{-1} and ~ 465 cm^{-1} are changing, which can be due to the contribution of the vibrations of Fe – O bonds of FeO_6 units [16, 17]. Also, with the addition of Fe_2O_3 in the glass matrix a new band at ~ 668 cm^{-1} due to the vibrations of Bi – O bonds of different lengths in BiO_6 polyhedra [9, 16 – 18] can be observed. Also, the contribution band of the vibrations of Fe – O bonds of FeO_4 units [16, 17] cannot be excluded. This band remains unchanged in all compositional range. These results suggest that the network structure of the $Bi_2O_3 \cdot CdO$ glass matrix is stable, and that Bi_2O_3 is the glass network former and CdO and Fe_2O_3 play the role of network modifiers.

The FT – IR spectra of $xFe_2O_3 \cdot (100\text{-}x)[Bi_2O_3 \cdot As_2O_3]$ glass system were studied starting from the FT – IR spectrum of $Bi_2O_3 \cdot As_2O_3$ glass matrix presented in Fig. 1. With the addition of iron ions (Fig. 4) the band from ~801 cm^{-1} and ~ 588 cm^{-1} are slowly decreasing. The band from ~ 421 cm^{-1} disappears for x = 0.5 mol % Fe_2O_3 instead a small band appears at ~ 463 cm^{-1} which is due to the contribution of the vibrations of Fe – O bonds of FeO_6 units [16, 18]. It slowly increases with the increasing of iron content. The addition of iron ions does not imply many changes in $Bi_2O_3 \cdot As_2O_3$ glass matrix. This suggests a high stability of the network structure formed in the glass matrix and a certain stability of the disorder order of the glasses. Due to the broadening of the bands it can not be exactly established the role played by Bi_2O_3 and As_2O_3.

The FT – IR spectra of $xFe_2O_3 \cdot (100\text{-}x)[Bi_2O_3 \cdot GeO_2]$ glass system were studied starting from the FT – IR spectrum of $Bi_2O_3 \cdot GeO_2$ glass matrix presented in Fig. 1. The addition of iron ions (Fig. 4) does not change the intensity and the shape of the band from ~ 874 cm^{-1}. The band from ~ 731 cm^{-1} is decreasing up to x = 50 mol %. The band from ~ 565 cm^{-1} is increasing and also a new band appears at ~ 464 cm^{-1} due to a contribution of the vibrations of Fe – O bonds of FeO_6 units [16, 17].

From FT – IR absorption of the glass systems studied it can be observed that the addition and increasing of iron ions do not imply major changes in the vitreous structure comparing with the vitreous matrices. Also the presence of iron ions was not directly evidenced.

3.3. Raman scattering data

The Raman spectra of $xFe_2O_3 \cdot (100\text{-}x)Bi_2O_3$ glass system present four absorption bands corresponding to the following wavenumber: ~ 601 cm^{-1}, ~ 377 cm^{-1}, ~ 127 cm^{-1} and ~ 85 cm^{-1} (Fig. 5). The low shoulder from ~ 601 $cm^{-1}$is assigned to Bi – O^- stretching vibrations of BiO_6 octahedral units [23, 30]. This shoulder is decreasing with the increasing of iron content and disapear for x = 10 mol%. The band from ~ 377 cm^{-1} is assigned to the Bi – O – Bi stretching vibrations of distorted BiO_6 octahedral units [23, 30]. This band is decreasing with the increasing of iron content. The bands from ~ 127 cm^{-1} and ~ 85 cm^{-1} are assumed to be derived from both AR and HM modes [27]. The Raman spectra confirm and complete the structure proposed by FT – IR spectra. It shows that the main structural units of the glass network are BiO_6 units and that the addition of iron ions leads to a progressively depolymerization of the glass network.

The Raman spectra of $xFe_2O_3 \cdot (100\text{-}x)[Bi_2O_3 \cdot CdO]$ glass system were studied starting from the Raman spectrum of $Bi_2O_3 \cdot CdO$ glass matrix presented in Fig. 2. With the addition of iron ions (Fig. 5) these bands are increasing up to 3 mol% and then decreases. For higher concentration of iron these bands disappear. That means that the addition of small contents of iron ions favorites the increasing of BiO_6 units. The addition of higher content of iron ions it leads to a depolymerization of the glass network.

The Raman spectra of $xFe_2O_3 \cdot (100\text{-}x)[Bi_2O_3 \cdot As_2O_3]$ glass system were studied starting from the Raman spectrum of $Bi_2O_3 \cdot As_2O_3$glass matrix presented in Fig. 2. With the addition and increasing of iron content (Fig. 5) the intensity are decreasing progressively up to 10 mol% and then disappears, leading to a depolymerization of the glass network structure. Same as FT – IR, the Raman measurement could not give a perspective of the role played by Bi_2O_3 and As_2O_3 in the glass network.

The Raman spectra of $xFe_2O_3 \cdot (100\text{-}x)[Bi_2O_3 \cdot GeO2]$ glass system were studied starting from the Raman spectrum of $Bi_2O_3 \cdot GeO_2$ glass matrix presented in Fig. 2. With the addition and increasing of iron ions the bands decrease up to 10 mol% and then disappear. Instead a new band appears at ~ 78 cm^{-1} which is assumed to be derived from both AR and HM modes [27]. The Raman spectra confirm that the addition of iron ions is leading to a depolymerization of the glasses.

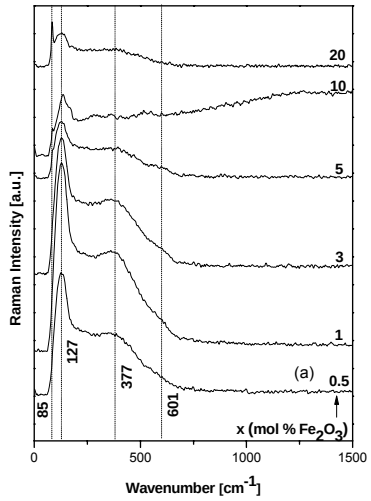

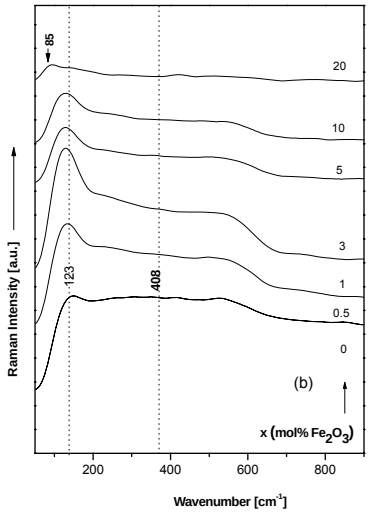

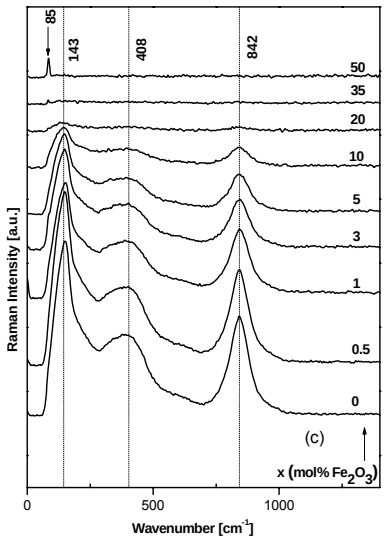

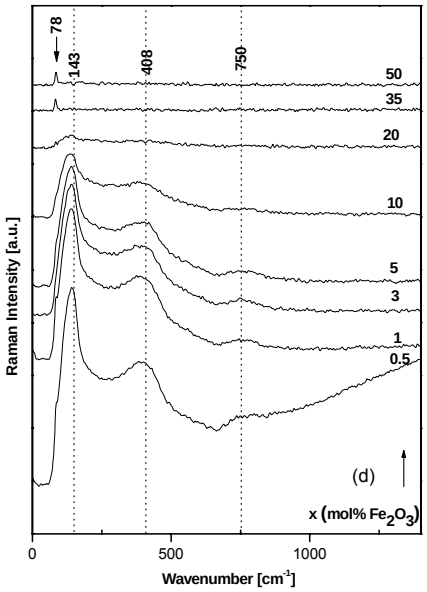

Fig. 5. Raman spectra of (a) $xFe_2O_3 \cdot (100\text{-}x)Bi_2O_3$, (b) $xFe_2O_3 \cdot (100\text{-}x)[Bi_2O_3 \cdot CdO]$ systems for $x \leq 20$ mol% and (c) $xFe_2O_3 \cdot (100\text{-}x)\ [Bi_2O_3 \cdot As_2O_3]$, (d) $xFe_2O_3 \cdot (100\text{-}x)[Bi_2O_3 \cdot GeO_2]$ systems for $x \leq 50$ mol%.

From Raman spectra it can be observed a progressively depolymerization of the vitreous systems studied with the increasing of iron content, which leads to a high disorder degree for higher content of iron.

4. Conclusions

Samples from $xFe_2O_3 \cdot (100\text{-}x)Bi_2O_3$ and $xFe_2O_3 \cdot (100\text{-}x)[Bi_2O_3 \cdot MO]$ systems (where MO ⟹ CdO, As_2O_3 and GeO_2), with $0.5 \leq x \leq 50$ mol%, were prepared and investigated by X-Ray diffraction, FT – IR and Raman spectroscopies in order to obtain information about their structure and to point out the role of each component of the glass system in the forming of the glass network.

From XRD patterns it was obtained:

- homogenous glasses for $x \leq 20$ mol% for $xFe_2O_3 \cdot (100\text{-}x)Bi_2O_3$ and $xFe_2O_3 \cdot (100\text{-}x)(Bi_2O_3 \cdot CdO)$ systems
- homogenous glasses for $x \leq 50$ mol% for $xFe_2O_3 \cdot (100\text{-}x)(Bi_2O_3 \cdot As_2O_3)$ and $xFe_2O_3 \cdot (100\text{-}x)(Bi_2O_3 \cdot GeO_2)$

From FT – IR spectra it was observed that $xFe_2O_3 \cdot (100\text{-}x)Bi_2O_3$ and $xFe_2O_3 \cdot (100\text{-}x)(Bi_2O_3 \cdot CdO)$ glass systems have the same behavior with the addition and increasing of iron content. Their structure is based mainly on BiO_6 units. The BiO_3 units are also observed in these systems.

The FT – IR spectra of $xFe_2O_3 \cdot (100\text{-}x)(Bi_2O_3 \cdot As_2O_3)$ suggests a structure built from BiO_6 and AsO_3 units, where, due to the broadness of the bands, a high disorder degree was suggested. The presence of BiO_3 units cannot be excluded.

The FT – IR spectra of $xFe_2O_3 \cdot (100\text{-}x)(Bi_2O_3 \cdot GeO_2)$ suggests a structure built from BiO_3, BiO_6 and GeO_4 units. A high disorder degree was observed also in this glass system due to the broad bands presented in the FT – IR spectra.

In all investigated glass systems the presence of Fe_2O_3 structural units was not directly evidenced but its presence cannot be excluded.

The Raman spectra sustain the information given by FT – IR spectra. By Raman spectroscopy only the presence of BiO_6 structural units was evidenced. With the increasing of iron content the BiO_6 structural units are smoothly decreasing. The addition and increasing of iron content causes a depolymerization of the investigated structures. The presence of structural units characteristic to iron ions was not directly evidenced by Raman spectroscopy.

References

[1] D. Hall, N. Newhause, N. Borrelli, W. Dumbaugh, D. Weidman, J. Appl. Phys. Lett. **54**, 1293 (1998).

[2] T. Komatsu, K. Matusita, Thermochim. Acta **174**, 131 (1991).

[3] H. Zheng, P. Lin, R. Xu, J. Mackenzie, J. Appl. Phys. **68**, 894 (1990).

[4] W. H. Dumbaugh, J. C. Lapp, J. Am. Soc. **75**, 2315 (1992).

[5] C. Laxmi Kanth , B. V. Raghavaiah, B. Appa Rao, N. Veeraiah, Journal of Quantitative Spectroscopy & Radiative Transfer **90**, 97 (2005).

[6] A. G. Clare, A. C. Wright, R. N. Sinclair, F. L. Galeener, A. E. Geissberger, J. Non – Cryst. Solids **111**, 123 (1989).

[7] K. Nassau, D. L. Chadwick, A.E. Miller, J. Non – Cryst. Solids **93**, 115 (1987).

[8] K. Nassau, D. L. Chadwick, J. Am. Ceram. Soc. **66**, 332 (1983).

[9] V. Dimitrov, Y. Dimitriev, A. Montenero, J. Non – Cryst. Solids **180**, 51 (1994).

[10] E. I. Kamitsos, Y. D. Yiannopoulos, M. A. Karakassides, G. D. Chryssikos, H. Jain, J. Phys. Chem. **100**, 11755 (1996).

[11] D. K. Durga, N. Veeraiah, Physica B **324**, 127 (2002).

[12] G. Srinivasarao, N. Veeraiah, J. Phys. Chem. Solids **63**, 705 (2002) 705.

[13] V. Rajendran, N. Palanivelu, B. K. Chaudhuri, K. Goswami, J. Non – Cryst. Solids **320**, 195 (2003).

[14] P. Tarte, Spectrochim. Acta **18**, 467 (1962).

[15] R. A. Condrate, J. Non – Cryst. Solids **84**, 26 (1986).

[16] R. Iordanova, Y. Dimitriev, V. Dimitrov, S. Kassabov, D. Klissurski, J. Non – Cryst. Solids **231**, 227 (1998).

[17] R. Iordanova, Y. Dimitriev, S. Kassabov, D. Klissurski, J. Non – Cryst. Solids **204**, 141 (1996).

[18] V. Dimitrov, Y. Dimitriev, A. Montenero, J. Non – Cryst. Solids **180**, 51 (1994).

[19] F. F. Bentley, L. D. Smithson, A. L. Rozek, Interscience, New York, 1968, p. 103.

[20] G. Lucovsky, F. L. Galeener, J. Non – Cryst. Solids **46**, 203 (1981).

[21] G. S. Rao, N. Veeraiah, J. Alloys Compd. **327**, 52 (2001).

[22] D. Sreenivasu, V. Chandramouli, Bull. Mater. Sci. **23**, 281 (2000).

[23] I. Ardelean, I. Todor, P. Pascuta, Mod. Phys. Lett. B **18**, 1 (2004).

[24] M. E. Lines, J. Non – Cryst. Solids **89**, 143 (1987).

[25] M. E. Lines, A. E. Miller, K. Nassau, K. B. Lyons, J. Non – Cryst. Solids **89**, 163 (1987).

[26] S. Hazra, S. Mandal, A. Gosh, Phys. Rev. B **56**, 8021 (1997).

[27] A. E. Miller, K. Nassau, K. B. Lyons, M. E. Lines, J. Non – Cryst. Solids **99**, 289 (1988).

[28] J. O. Jensen, S. J. Gilliam, A. Banerjee, D. Zeroka, S. J. Kirkby, C. N. Merrow, J. Mol. Struct. (Theochem), **664 – 665**, 145 (2003).

[29] P. B. Benventi, D. Bersani, P. P. Lottici, L. Kovacs, F. Cordioli, A. Montenero şi G. Gnappi, J. Non-Crist. Solids, **192&193**, 258 (1995).

[30] P. P. Lottici, G. Antonioli, C. Razzetti, A. Montenero, Phys. Non – Cryst. Solids, Ed. by L. D. Pze et al., Taylor and Francis, London, 1992, p.101.

[31] A. A. Kharlamov, R. M. Almeida, J. Heo, J. Non – Cryst. Solids **202**, 233 (1996).

* Corresponding author: arde@phys.ubbcluj.ro